# Beam Splash Mitigation for NGSO Spectrum Coexistence between Feeder and User Downlink

Eva Lagunas*, Ana Pérez-Neira†‡§, Joel Grotz¶, Symeon Chatzinotas* and Bjorn Ottersten*
*SnT - University of Luxembourg, Luxembourg
†Centre Tecnologic de Telecomunicacions de Catalunya (CTTC/CERCA), Castelldefels, Spain
‡ICREA Academia
§Universitat Politecnica de Catalunya (UPC), Barcelona, Spain
¶SES S.A., Luxembourg
Corresponding Author: eva.lagunas@uni.lu

***Abstract*—Non-geostationary (NGSO) satellite systems face a significant number of technical challenges when compared to conventional GSO systems, the most critical being the satellite mobility. The time-varying projection of the satellite spot-beam over the target area, i.e. the beam splash, may overlap with neighboring beams and result in inter-beam interference when those beam share the same spectrum. Given the large number of gateways needed to feed a NGSO constellation, and the common requirement of satellite customers to have gateway close to the end-users, it is expected to have beam splash effect between feeder and user downlinks. The main goal of this paper is to shed light on this rather unexplored coexistence scenario by providing link budget analysis and proposing beam-nulling solutions to mitigate the potential risk of interference.**

***Index Terms*—Spectrum sharing, Satellite Communications, NGSO constellation, Beamforming**

## I. Introduction

High-speed broadband internet from space represents a promising solution to provide coverage to the 45% of households on Earth that still lack internet access [1]. Most of the unconnected world can be related to low-income countries and/or remote areas with difficult terrain. Furthermore, a space-based access can be preferred for moving platforms, which can reduce the frequent terrestrial handover during the moving path. The idea of enveloping the planet with a large constellation of small low-orbiting satellites has gained momentum as a low-cost and low-latency alternative compared to the Geostationary (GSO) satellite systems. The most ambitious projects of this kind are represented by the American SpaceX [2], the British OneWeb [3] and the Luxembourgish SES mPower [4], all three of them in a mix of development, launching and preliminary operation.

Non-geostationary (NGSO) satellite systems face a significant number of technical challenges when compared to conventional GSO systems. First and foremost, satellites move across the sky claiming for more advanced User Terminals (UT) able to track this movement over time and execute seamless handover when the satellite disappears from the field of view. Furthermore, large constellations generally require a complex ground network with a significant number of gateways strategically distributed so as to ensure feeder link coverage to all satellites with high availability.

The gateway feeder links are served using similar pencil-beam as used for the user terminals. In fact, operational gateway feeder links for NGSO high-throughput systems typically operate in Ka-band, the same used by the user terminals [1]. Focusing on the Ka-band downlink, we have between 17.7 GHz and 20.2 GHz whose 2.5 GHz bandwidth is fully exploited by the gateway feeder downlink to aggregate the traffic from multiple user terminals. The user terminals and corresponding single-carrier beams work on the same spectrum but generally with much lower bandwidth, i.e. $\sim$200 MHz.

Increasingly, satellite customers require to have the gateway ground stations closer to them (e.g. in the same country or in friendly territory). However, the unavoidable spectrum sharing with the data-hungry feeder downlinks may limit the deployment of user terminals around the gateway locations. As an example, Fig. 1 shows two pencil-like beams from the same Medium Earth Orbit (MEO) satellite. Although the beams are circular conceived, there is an evident beam splash caused by the projection of the circular beam on the target area of the globe. In Fig. 1(a), the satellite is entering the field of view from the West and there is a minor beam overlap; while in Fig. 1(b), which is some minutes later, the beam overlap is significant.

The problem gets aggravated by the time-varying projection of the beam over the target area. In other words, depending on the geometry of the problem, the interference may increase or decrease over time. Clearly, there is a tolerable interference level that shall not be exceeded. Otherwise, different solutions may be considered, such as: (i) hand-over user terminal to another satellite; (ii) power control to keep a minimum spectral efficiency; (iii) beamforming (changing the pencil-beam form). Note that the solution of placing the gateway far

[1] Although there are prospects of exploiting Q/V band [5], the technology is not yet mature enough and requires a very dense ground network deployment to counteract weather impairments.

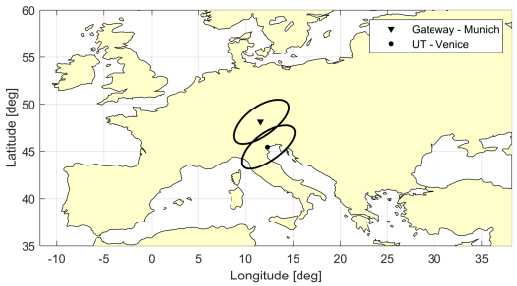


(a) MEO at longitude -16.7 degree

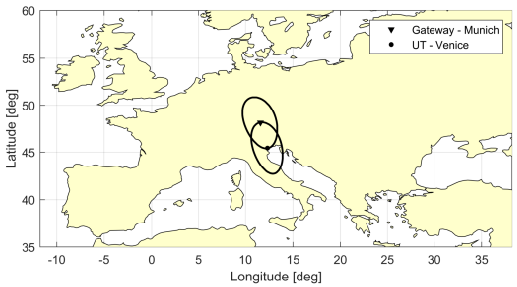


(b) MEO at longitude 19.3230 degree

Fig. 1. Example of 2 MEO beams with a beam border indicating the -3dB beam gain region. The MEO satellite is at the equatorial plane. Beam generated following 3GPP-Rel15 [6].

from the final users is in some cases not a valid option for security reasons.

The main goal of this paper is to shed some light on this rather new coexistence issue that has emerged with the new age of NGSO satellite constellations, which bring mobility as a technical challenge with respect to their GSO counterpart. In particular, we do link budgeting exercise based on realistic scenario deployment which demonstrate the spectrum coexistence problem. Furthermore, we propose an adaptive beamforming design with a null-steering direction towards the victim. The efficiency of the proposed method and its practical constraints in terms of speed of update are illustrated via numerical simulations.

The remainder of the paper is organized as follows. Section II presents the system model. Section III presents the main contribution of this paper. The simulation results are presented in Section IV. Finally, Section V concludes the paper.

*Notations*: Throughout the paper, a capital bold letter such as $\mathbf{A}$ represents a matrix, and a lower case bold letter $\mathbf{a}$ represents a vector. The superscripts have the following meanings: $(\cdot)^H$ is the conjugate transpose of a matrix, and $(\cdot)^{-1}$ is matrix inversion.

## II. System Model

For the sake of simplicity of the analysis, we consider the downlink from one NGSO satellite towards two ground stations, one representing a GW and one representing a UT. Both ground stations are relatively close to each other at a distance $\ell_{\text{dist}}$. The GW is assumed to operate in Ka-band expanding on the whole available spectrum between 17.7 GHz and 20.2 GHz. Note that GWs typically collect and manage all the traffic of multiple UT distributed in the surrounding geographical area and, therefore, are bandwidth-hungry by nature. On the other hand, deployment of gateways is expensive and, as a consequence, satellite operators try to minimize its number while maximizing their usage. The bandwidth of the GW downlink is denoted by $B_{\text{total}} = 2$ GHz. On the other hand, the UT is assumed to operate in the same spectrum but with reduced bandwidth of $B_{\text{UT}} = 200$ MHz.

A NGSO satellite is providing coverage to both ground stations by allocating them separate pencil-type beams. In principle, such narrow beam-pattern should avoid interference between beams (see Fig. 1(a)). However, when distance $\ell_{\text{dist}}$ is small, the pencil-type beam "splashes" and potentially expands towards unwanted directions, causing potential overlapping between beams (see Fig. 1(b)).

The visibility-window of a NGSO satellite corresponding to a terminal $k$ on the Earth's surface can be expressed as $[T_{0,k}, T_{\text{end},k})$. During the visibility window, one beam is assigned to each ground terminal, with the beam center located on the intended user. In our study, we assume two ground terminals and, therefore, we consider the NGSO travelling time between $[\min(T_{0,k_1}, T_{0,k_2}), \max(T_{\text{end},k_1}, T_{\text{end},k_12})]$.

When the NGSO satellite is visible for ground terminal $k$, his intended received signal power is given by,

$$S_k^{\text{d}} \text{ [dBW]} = \text{EIRPSD}_{k,\max} \text{ [dBW/Hz]} \cdot \text{BW}_k \text{ [Hz]} + \\ + \text{PL}(k, f_k) \text{ [dB]} + G_{k,\max} \text{ [dBi]} \quad (1)$$

where,

- $\text{EIRPSD}_{k,\max}$ denotes the maximum Equivalent Isotropic Radiated Power Spectral Density (EIRPSD) at the beam allocated to user $k$, which occurs at the beam center.
- $\text{BW}_k$ is the operational bandwidth of the ground terminal $k$.
- $\text{PL}(k, f_k)$ denotes the free-space Path Loss (PL) towards the $k$ ground station operating at central frequency $f_k$.
- $G_{k,\max}$ denotes the maximum antenna gain at reception for ground terminal $k$ which occurs at the boresight direction and is given by,

$$G_{k,\max} = A_{\text{eff}} \left( \frac{\pi D_k}{\lambda} \right)^2 \quad (2)$$

where $D_k$ denotes the diameter of the antenna at receiver $k$ and $A_{\text{eff}}$ is the antenna efficiency.

Following the 2 closely-located ground terminals example, each ground receiver $k$ will be interfered by the adjacent beam

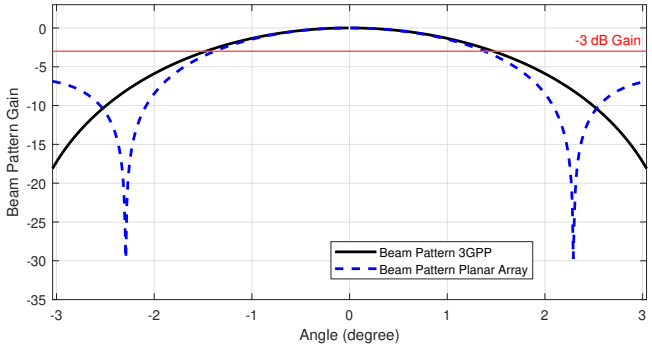


Fig. 2. Main beam generated with a 50 × 50 element DRA and compared to the 3GPP model.

$j$ with the following interference signal power:

$$S^{\mathrm{i}}_{k,j}\ [\mathrm{dBW}] = \mathrm{EIRPSD}_{j,k}\ [\mathrm{dBW/Hz}] \cdot \mathrm{BW}_j\ [\mathrm{Hz}] + \\ + \mathrm{PL}(k, f_j)\ [\mathrm{dB}] + G_{k,\max}\ [\mathrm{dBi}] + \\ + 10\log_{10}\left(\min\left(1, \frac{\mathrm{BW}_j}{\mathrm{BW}_k}\right)\right) \quad (3)$$

where $\mathrm{EIRPSD}_{j,k}$ denotes the EIRPSD that is emitted from the beam of user $j$ towards the location of user $k$. The last term in (3) quantifies the portion of the interferer bandwidth that overlaps with that from the ground receiver $k$.

As Key Performance Indicator (KPI) to identify whenever the link is at risk, we make use of the Carrier-over-Interference Ration (C/I), which is defined as follows,

$$C/I\ [\mathrm{dB}] = 10\log\left(S^{\mathrm{d}}_k / S^{\mathrm{i}}_{k,j}\right) \quad (4)$$

### A. Satellite Beam Pattern

A direct radiating phased array (DRA) antenna based on planar array is assumed to be mounted on the satellite system, capable to generate a beam pattern as shown in Fig. 2. The DRA pattern is compared with the reflector-aided circular antenna pattern mentioned in 3GPP Release 15 [6] and it can be observed that both patterns have a similar main beam with a -3 dB cut at 1.5° for 3GPP and 1.4° for the DRA one.

Fig. 3(a) shows the projection of the DRA-generated beam pattern when centered over the gateway location in Munich, Germany. It can be observed that the close-by UT falls within the main beam.

## III. Beam Splash Mitigation: Adaptive Beamforming

With the aim to maximize on-orbit flexibility, modern high-throughput satellites are equipped with programmable beamforming networks (BFN) [7].

A "fixed" BFN is in most of the cases selected for operation, which generate time-invariant spot beams with fixed beam center during the NGSO satellite pass. The "fixed" BFN is typically obtained with a Phased Array (PA) beamformer, where the goal is to preserve maximum gain towards a specific latitude and longitude coordinates while minimizing the radiated power. The PA beamformer design can be mathematically expressed as[2],

$$\begin{aligned} \min_{\mathbf{a}} \quad & \mathbf{a}^H\mathbf{a} \\ \text{s.t.} \quad & \mathbf{a}^H\mathbf{s}_d = 1, \end{aligned} \quad (5)$$

where $\mathbf{a} = \frac{\mathbf{s}_d}{N}$ denotes the PA beamforming vector and $\mathbf{s}_d \in \mathbb{C}^{1\times N}$ denotes the steering vector towards the desired angle (i.e. towards the desired latitude and longitude).

The PA design corresponds to the beam projections illustrated in Fig. 3. Note that the BFN needs to update regularly the beamforming design by correcting the beam pointing ($\mathbf{s}_d$ changes with the NGSO movement). Furthermore, this design does not take into account neighboring ground stations and potential beam overlap between them.

Typically, the link quality is constantly monitored by the satellite system by checking the $C/I$ [dB] (4). In particular, the $C/I$ is compared to a predetermined threshold $(C/I)_{\mathrm{thr}}$:

$$\begin{aligned} &\text{Link is at risk :} \quad (C/I) < (C/I)_{\mathrm{thr}}, \\ &\text{Link has no risk :} \quad (C/I) \geq (C/I)_{\mathrm{thr}}, \end{aligned} \quad (6)$$

To avoid undesired link degradation due to the beam splash problem illustrated in Fig. 1, we propose to modify the BFN during the beam tracking mode by taking into account the known locations of the ground sites suffering from interference. The latter can be easily introduced to (5) by adding one new constraint for each unintended steering angle:

$$\begin{aligned} \min_{\mathbf{a}} \quad & \mathbf{a}^H\mathbf{a} \\ \text{s.t.} \quad & \mathbf{C}^H\mathbf{a} = \mathbf{f}, \end{aligned} \quad (7)$$

where $\mathbf{f} = \begin{bmatrix}1 & 0 & \cdots & 0\end{bmatrix}^T$ and $\mathbf{C} = \begin{bmatrix}\mathbf{s}_d & \mathbf{s}_1 & \cdots & \mathbf{s}_{K-1}\end{bmatrix}$ is the constraint matrix with $\mathbf{s}_i$, $i = 1, \ldots, K$, being the array response vectors towards the interfering directions. Note that the number of constraints must be smaller than the number of antenna elements, otherwise the problem would be over-determined. The solution to (7) is given by,

$$\mathbf{a} = \mathbf{C}\left(\mathbf{C}^H\mathbf{C}\right)^{-1}\mathbf{f}. \quad (8)$$

The expression in (8) corresponds to the zero-forcing precoding, which has been considered in the past mostly for geostationary satellite systems and with implementation at ground segment [8], [9] (not on the satellite antenna).

### A. How fast shall the BFN be updated?

Beam management plays a key role in an efficient satellite mobility management, and we can distinguish the acquisition and the tracking phase. The former consists in finding the best satellite beam for each UT and the scanning must be within the satellite pass. The latter consists in tracking the satellite

[2]We assume an $N$-element linear array notation for the sake of simplicity. The notation can be easily extended to the planar array context.

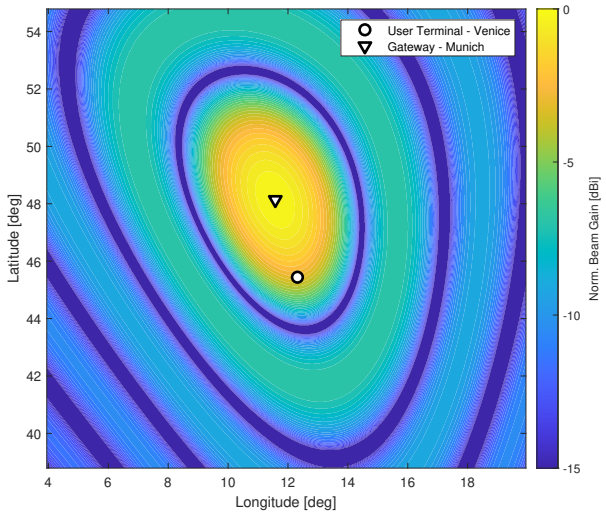


(a) PA response: UT gain -2.94 dBi

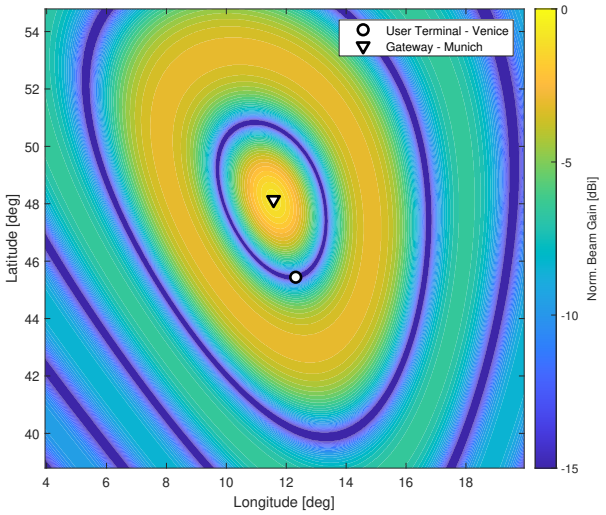


(b) Nulling towards UT: UT gain -26.78 dBi

Fig. 3. Beam projection for MEO at 19.32 E

movement from a perfectly pointed beam. The proposed constrained beamformer in (7) is for the tracking phase.

In terms of user experience, it is clear that the faster the BFN adapts to the satellite movement, the better. However, there exists limitations in terms of operations and latency in terms of execution. Recalculating the beamformer vectors implies executing a number of operations, which is typically done on-ground for the sake of preserving power of the spacecraft. The design is then communicated to the satellite via signalling and then the payload executes the beamforming update. All this procedure takes time and there exists a clear trade-off between user experience and overhead in terms of computational complexity (to calculate the design) and signalling.

The aim of this paper is to carry out a preliminary study of the impact of beam splash in NGSO satellites for downlink spectrum coexistance and evaluate how a basic beamforming nulling capabilities can help. The research of beamforming design that can adapt to the NGSO scenario is left for future work.

## IV. Numerical Evaluation

In this section, we evaluate the impact of the beam splash problem for a specific scenario with 1 GW and 1 UT similar as the scenario depicted in Fig. 1 and Fig. 3.

### A. Simulation Setup

We assume a GW station and a UT station with coordinates as indicated in Table I. AGI's Satellite Toolkit (STK) is used to extract the exact orbital propagation of one SES mPower satellite in MEO orbit [4]. We focus on one single MEO pass over the area of the GW and UT location, which starts at 13:44:42 of the 31 Jul 2022 and ends at 15:27:13 of the same day. Munich *sees* the MEO for during approx. 97 minutes while Venice *sees* MEO for approx. 103 minutes. We take snapshots at 1 minutes time interval for our evaluation.

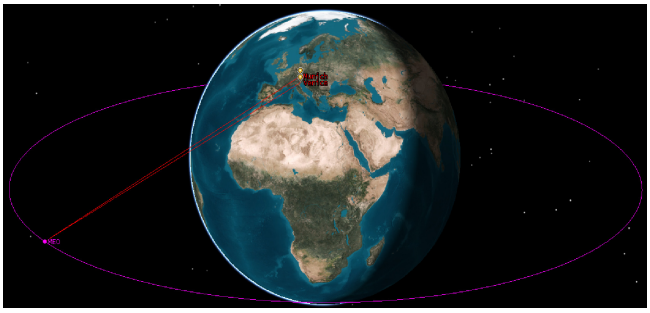

Fig. 4. Scenario from AGI STK Toolkit

The considered system parameters are summarized in Table II and the scenario simulated in AGI STK toolkit is illustrated in Fig. 4.

TABLE I
Geographical Coordinates

| | **Latitude** | **Longitude** |
|---|---|---|
| **GW (Munich, Germany)** | 48.13715 | 11.576124 |
| **UT (Venice, Italy)** | 45.4408 | 12.3155 |

### B. Numerical Results

As initial exercise, Fig. 3 compares a particular snapshot with and without beam nulling, in this case from the GW towards the UT. It can be observed that the UT achieves a reduction of -23.84 dBi in terms of interference by using the propose beamforming in (7).

TABLE II
SIMULATION PARAMETERS

| Parameter | Value |
|---|---|
| MEO orbit | Equatorial |
| MEO altitude | 8062 Km |
| MEO period | 6 hours |
| Operational frequency | 19.5 GHz |
| EIRPSD satellite | -48 dBW |
| Planar Array (square) | N=50 elements |
| Bandwidth GW link | 2 GHz |
| Diameter GW dish | 3.5 meters |
| Bandwidth UT link | 200 MHz |
| Diameter UT dish | 0.6 meters |
| Min. Elevation | 10° |
| RX Antenna Efficiency | 0.6 |

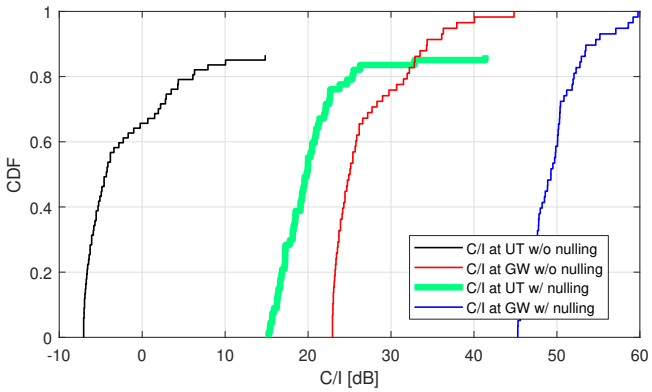


Fig. 5. CDF of C/I metric with and without advanced beamforming design.

To have the full picture of the overall MEO pass over the region of interest, Fig. 5 shows the cumulative distribution function (CDF) of the C/I metric as defined in (4) for both the GW and the UT, considering a simple PA (without nulling) and the proposed beamforming with nulling. The benefits in terms of C/I improvement are evident, particularly for the UT case, which operates in a smaller spectrum and with lower power than the GW counterpart.

Fig. 6 illustrates the evolution over time of the C/I metric. Considering a $(C/I)_{\text{thr}}$ threshold of 15 dB, it becomes evident that the link of UT is constantly at risk unless we apply some mitigation technique, while the GW is out of risk for the whole satellite pass. The later is justified by the difference of bandwidths $\text{BW}_{GW} \gg \text{BW}_{UT}$. Note that Fig. 6 emulates a simplistic scenario with a single UT with relatively low bandwidth. The impact of multiple UT aggregating interference at the GW could benefit from the proposed beamforming. Following with the UT behavior at Fig. 6, we can observe that applying the adaptive beamforming "moves" the UT links above the C/I threshold.

Finally, Table III evaluates the C/I metric versus the beam updating speed, i.e. how often we recalculate the beam in (7). As expected, in terms of performance, the best is to updated instantaneously. Table III shows that the C/I degrades as soon as we do not instantaneously update the beam nulling, with

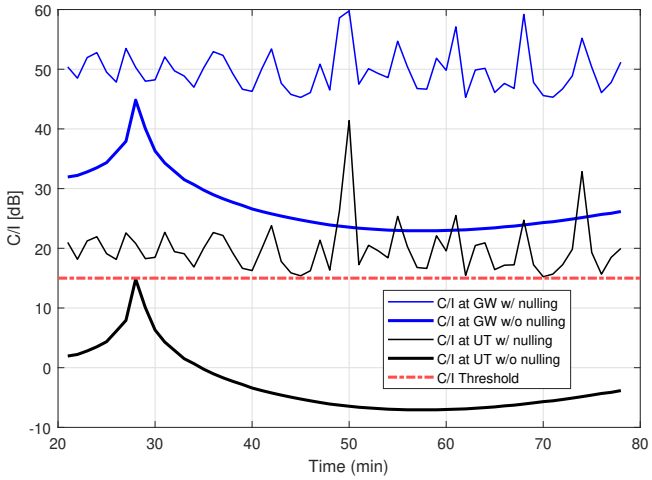


Fig. 6. Instantaneous C/I metric with and without advanced beamforming design.

TABLE III
C/I VERSUS BEAM UPDATING SPEED

| | | Instantaneous | 2 min | 5 min |
|---|---|---|---|---|
| **GW** | **PA** | 27.13 dB | | |
| | **BFN Nulling** | 49.71 dB | 44.26 dB | 38.06 dB |
| **UT** | **PA** | -2.87 dB | | |
| | **BFN Nulling** | 19.91 dB | 14.52 dB | 8.20 dB |

a ∼25% reduction for the GW case and a ∼60% reduction for the UT case if we consider updates every 5 minutes.

## V. CONCLUSIONS

In this paper, we considered a novel interference scenario that is expected to have a strong impact in future NGSO deployments, particularly for high throughput satellites with GWs making use of the whole available spectrum. We have shown the so-called "beam splash" concept, i.e. the expansion towards unwanted directions of the pencil-type beam projections on Earth. To overcome this issue, we have proposed to exploit the satellite BFN by designing a dynamic beamforming to minimize the interference towards known geographical locations. Results based on computer simulations are presented, which show the performance improvement when considering the proposed solution.

Although the study presented in the paper is very preliminary, it addressed a topic that will become highly relevant for the design of future NGSO satellite systems, particularly for dense LEO constellations. Future work include the extension to LEO scenario and the generalization to multiple UT.

## ACKNOWLEDGMENT

This work has been partially supported by the Luxembourg National Research Fund (FNR) under the project MegaLEO (C20/IS/14767486), by the Spanish ministry of science and innovation under project IRENE (PID2020-115323RB-C31)

funded by MCIN/AEI/10.13039/501100011033, and also by the ICREA Academia program funded by the Catalan government. Please note that the views of the authors of this paper do not necessarily reflect the views of SES S.A..

## REFERENCES

[1] "UNESCO Report: The State of Broadband 2019," https://www.itu.int/dms_pub/itu-s/opb/pol/S-POL-BROADBAND.20-2019-PDF-E.pdf, accessed: 2022-08.

[2] "Space Exploration Technologies Corp." https://www.spacex.com/, accessed: 2022-08.

[3] "OneWeb," https://oneweb.net/, accessed: 2022-08.

[4] "SES mPower," https://www.ses.com/o3b-mpower, accessed: 2022-08.

[5] M. Aloisio, P. Angeletti, F. Coromina, and R. De Gaudenzi, "Exploitation of Q/V-band for future broadband telecommunication satellites," in *IVEC 2012*, 2012, pp. 351–352.

[6] "3GPP TR 38.811 V15.4.0 (2020-09) [Online]," https://www.3gpp.org/release-15, accessed: 2022-08.

[7] G. Toso, P. Angeletti, and C. Mangenot, "Multibeam antennas based on phased arrays: An overview on recent ESA developments," in *The 8th European Conference on Antennas and Propagation (EuCAP 2014)*, 2014, pp. 178–181.

[8] P.-D. Arapoglou *et al.*, "DVB-S2X-enabled precoding for high throughput satellite systems," *International Journal of Satellite Communications and Networking (IJSCN)*, vol. 34, no. 3, pp. 439–455, 2016. [Online]. Available: https://onlinelibrary.wiley.com/doi/abs/10.1002/sat.1122

[9] M. A. Vazquez, A. Perez-Neira, D. Christopoulos, S. Chatzinotas, B. Ottersten, P. Arapoglou, A. Ginesi, and G. Taricco, "Precoding in Multibeam Satellite Communications: Present and Future Challenges," *IEEE Wireless Communications*, vol. 23, no. 6, pp. 88–95, December 2016.